0022-3565/11/3363-940–951$20.00
THE JOURNAL OF PHARMACOLOGY AND EXPERIMENTAL THERAPEUTICS
JPET 336:940–951, 2011

Vol. 336, No. 3
175117/3671515
*Printed in U.S.A.*

# meso-Transdiene Analogs Inhibit Vesicular Monoamine Transporter-2 Function and Methamphetamine-Evoked Dopamine Release[S]

David B. Horton, Kiran B. Siripurapu, Seth D. Norrholm, John P. Culver, Marhaba Hojahmat, Joshua S. Beckmann, Steven B. Harrod,[1] Agripina G. Deaciuc, Michael T. Bardo, Peter A. Crooks, and Linda P. Dwoskin

*Department of Pharmaceutical Sciences, College of Pharmacy (D.B.H., K.B.S., S.D.N., J.P.C., M.H., A.G.D., P.A.C., L.P.D.), and Department of Psychology, College of Arts and Sciences (J.S.B., S.B.H., M.T.B.), University of Kentucky, Lexington, Kentucky*

Received September 13, 2010; accepted December 16, 2010

**ABSTRACT**

Lobeline, a nicotinic receptor antagonist and neurotransmitter transporter inhibitor, is a candidate pharmacotherapy for methamphetamine abuse. meso-Transdiene (MTD), a lobeline analog, lacks nicotinic receptor affinity, retains affinity for vesicular monoamine transporter 2 (VMAT2), and, surprisingly, has enhanced affinity for dopamine (DA) and serotonin transporters [DA transporter (DAT) and serotonin transporter (SERT), respectively]. In the current study, MTD was evaluated for its ability to decrease methamphetamine self-administration in rats relative to food-maintained responding. MTD specifically decreased methamphetamine self-administration, extending our previous work. Classical structure-activity relationships revealed that more conformationally restricted MTD analogs enhanced VMAT2 selectivity and drug likeness, whereas affinity at the dihydrotetrabenazine binding and DA uptake sites on VMAT2 was not altered. Generally, MTD analogs exhibited 50- to 1000-fold lower affinity for DAT and were equipotent or had 10-fold higher affinity for SERT, compared with MTD. Representative analogs from the series potently and competitively inhibited [$^3$H]DA uptake at VMAT2. (3*Z*,5*Z*)-3,5-bis(2,4-dichlorobenzylidene)-1-methylpiperidine (UKMH-106), the 3*Z*,5*Z*-2,4-dichlorophenyl MTD analog, had improved selectivity for VMAT2 over DAT and importantly inhibited methamphetamine-evoked DA release from striatal slices. In contrast, (3*Z*,5*E*)-3,5-bis(2,4-dichlorobenzylidene)-1-methylpiperidine (UKMH-105), the 3*Z*,5E-geometrical isomer, inhibited DA uptake at VMAT2, but did not inhibit methamphetamine-evoked DA release. Taken together, these results suggest that these geometrical isomers interact at alternate sites on VMAT2, which are associated with distinct pharmacophores. Thus, structural modification of the MTD molecule resulted in analogs exhibiting improved drug likeness and improved selectivity for VMAT2, as well as the ability to decrease methamphetamine-evoked DA release, supporting the further evaluation of these analogs as treatments for methamphetamine abuse.

## Introduction

Methamphetamine abuse is a serious public health concern (Substance Abuse and Mental Health Services Administration, Office of Applied Studies, 2008). Pharmacotherapies are not available to treat methamphetamine abuse. Efforts have focused on the dopamine (DA) transporter (DAT) as a therapeutic target (Dar et al., 2005; Howell et al., 2007; Tanda et al., 2009), because methamphetamine interacts with DAT to increase extracellular DA concentrations, leading to its reinforcing properties (Wise and Bozarth, 1987; Di Chiara and Imperato, 1988; Di Chiara et al., 2004). DAT translocates DA from the extracellular space into presynaptic terminals, whereas methamphetamine reverses DAT translocation to increase DA extracellularly (Fischer and Cho, 1979; Liang and Rutledge, 1982; Sulzer et al., 1995). The above approach has not led to therapeutic agents for methamphetamine abuse, although several DAT inhibitors currently are undergoing clinical trials.

A largely unexplored target of methamphetamine action is vesicular monoamine transporter 2 (VMAT2). By interacting with VMAT2, methamphetamine increases cytosolic DA concentrations available for translocation by DAT to the extra-

This work was supported by the National Institutes of Health National Institute on Drug Abuse [Grants DA 13519, DA 016176, DA 021287].

The University of Kentucky holds patents on the analogs described, and some of the patents have been licensed by Yaupon Therapeutics, Inc. A potential royalty stream to L.P.D. and P.A.C. may occur consistent with University of Kentucky policy. Both L.P.D. and P.A.C. are founders of, and have financial interest in, Yaupon Therapeutics, Inc.

[1] Current affiliation: Department of Psychology, Behavioral Neuroscience Program, University of South Carolina, Columbia, South Carolina.

Article, publication date, and citation information can be found at http://jpet.aspetjournals.org.

doi:10.1124/jpet.110.175117.

[S] The online version of this article (available at http://jpet.aspetjournals.org) contains supplemental material.

cellular compartment (Sulzer and Rayport, 1990; Pifl et al., 1995; Sulzer et al., 1995). Current research focuses on the discovery of novel compounds that interact with VMAT2 and inhibit the pharmacological effects of methamphetamine. Lobeline, the major alkaloid of *Lobelia inflata*, inhibits VMAT2 function (Teng et al., 1997, 1998), has high affinity for [$^3$H]dihydrotetrabenazine (DTBZ) binding sites on VMAT2 (Kilbourn et al., 1995; Miller et al., 2004), and decreases amphetamine-evoked DA release from rat striatal slices (Miller et al., 2001). However, lobeline is not selective for VMAT2, acting as a nicotinic acetylcholine receptor (nAChR) antagonist with low affinity for DAT and the serotonin transporter (SERT) (Damaj et al., 1997; Flammia et al., 1999; Miller et al., 2000, 2004). Lobeline also decreases methamphetamine-induced hyperactivity, behavioral sensitization, and self-administration in rats (Harrod et al., 2001; Miller et al., 2001). It is noteworthy that lobeline is not self-administered, indicating lack of abuse liability (Harrod et al., 2003). Based on these preclinical findings, lobeline is being evaluated as a treatment for methamphetamine abuse. Initial-phase clinical trials report that lobeline is safe in methamphetamine addicts (http://www.clinicaltrials.gov/ct2/show/NCT00439504?term=NCT00439504&rank=1).

Lobeline has a central piperidine ring with phenyl rings attached at C-2 and C-6 of the piperidine ring by ethylene linkers containing hydroxyl and keto functionalities at the C8 and C10 positions on the linkers, respectively (Fig. 1). Potency and selectivity for VMAT2 were improved based on structure-activity relationships (SARs), with the emergence of two new lead compounds, i.e., lobelane and meso-transdiene (MTD) (Zheng et al., 2005; Nickell et al., 2010a). Lobelane is a lobeline analog with defunctionalized (hydroxyl and keto groups of lobeline eliminated from the linkers) and saturated linkers. Subsequent reports described the preclinical evaluation of lobelane as well as analogs based on the lobelane structural scaffold (Beckmann et al., 2010; Nickell et al., 2010b). MTD is a lobeline analog with defunctionalized and unsaturated (double bonds) linkers (Fig. 1). Compared with lobeline, MTD was found to exhibit similar affinity for the [$^3$H]DTBZ binding site on VMAT2 and decreased affinity for nAChRs, thus revealing increased selectivity for VMAT2 (Zheng et al., 2005). In addition, MTD inhibited methamphetamine-evoked DA overflow from rat striatal slices (Nickell et al., 2010a). However, MTD exhibited high affinity for DAT (Miller et al., 2004), which has been associated with the potential for abuse liability. Furthermore, MTD has limited solubility, diminishing its potential for development as a pharmacotherapy for methamphetamine abuse.

To extend the previous work, the current study determined whether MTD decreases methamphetamine self-administration in rats. The current SAR also identified analogs based on the MTD scaffold that potently and selectively inhibit VMAT2 function and had both low affinity for DAT and increased water solubility compared with MTD. These analogs were designed as more rigid, conformationally restricted

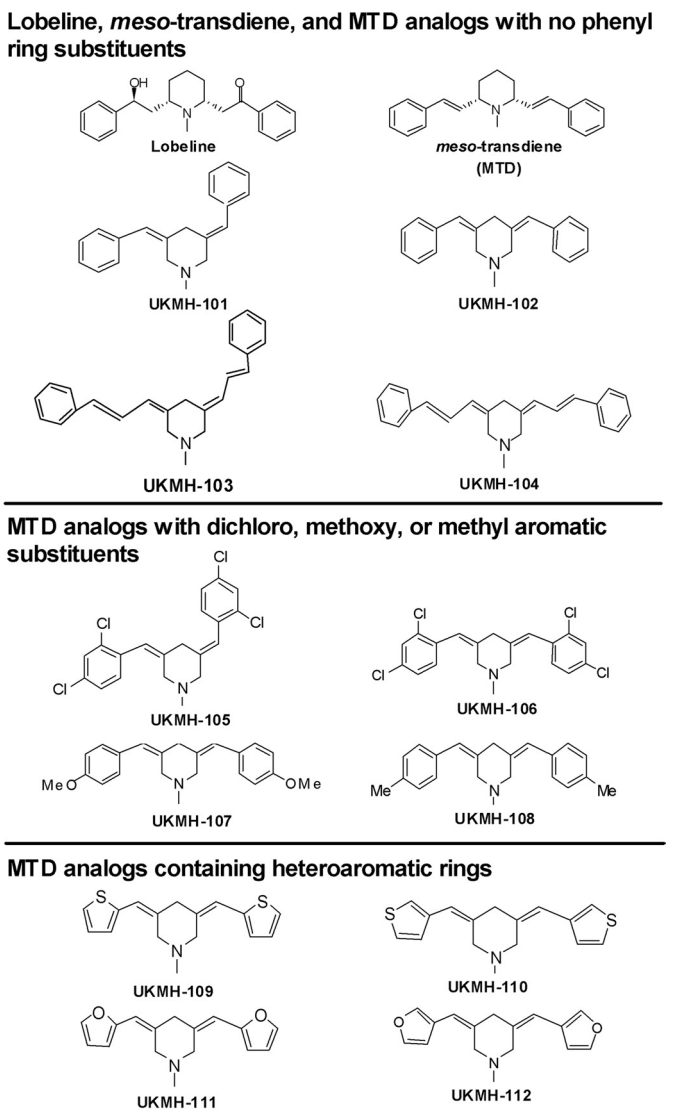


**Fig. 1.** Chemical structures of lobeline, MTD, and MTD analogs incorporating the phenylethylene moiety of MTD into the piperidine ring system with the addition of various phenyl ring substituents. For clarity of presentation, compounds are grouped according to structural similarity. Top, lobeline, MTD, and MTD analogs with no phenyl ring additions. Middle, MTD analogs with dichloro, methoxy, or methyl additions. Bottom, MTD analogs with heteroaromatic phenyl ring substitutions.

**ABBREVIATIONS:** DA, dopamine; DAT, DA transporter; 5-HT, 5-hydroxytryptamine (serotonin); ANOVA, analysis of variance; DOPAC, dihydroxyphenylacetic acid; DTBZ, dihydrotetrabenazine; GBR 12909, 1-(2-(bis-(4-fluorophenyl)methoxy)ethyl)-4-(3-phenylpropyl)-piperazine; MLA, methyllycaconitine; MTD, meso-transdiene; nAChR, nicotinic acetylcholine receptor; PEI, polyethyleneimine; Ro-4-1284, (2*R*,3*S*,11b*S*)-2-ethyl-3-isobutyl-9,10-dimethoxy-2,2,4,6,7,11b-hexahydro-1*H*-pyrido[2,1-a]isoquinolin-2-ol; SAR, structure-activity relationship; SERT, serotonin transporter; UKMH-101, (3*Z*,5*E*)-3,5-dibenzylidene-1-methylpiperidine; UKMH-102, (3*Z*,5*Z*)-3,5-dibenzylidene-1-methylpiperidine; UKMH-103, (3*Z*,5*E*)-1-methyl-3,5-bis((*E*)-3-phenylallylidene)piperidine; UKMH-104, (3*Z*,5*Z*)-1-methyl-3,5-bis((*E*)-3-phenylallylidene)piperidine; UKMH-105, (3*Z*,5*E*)-3,5-bis(2,4-dichlorobenzylidene)-1-methylpiperidine; UKMH-106, (3*Z*,5*Z*)-3,5-bis(2,4-dichlorobenzylidene)-1-methylpiperidine; UKMH-107, (3*Z*,5*Z*)-3,5-bis(4-methoxybenzylidene)-1-methylpiperidine; UKMH-108, (3*Z*,5*Z*)-1-methyl-3,5-bis(4-methylbenzylidene)-piperidine; UKMH-109, (3*Z*,5*Z*)-1-methyl-3,5-bis(thiophen-2-ylmethylene)piperidine; UKMH-110, (3*Z*,5*Z*)-1-methyl-3,5-bis(thiophen-3-ylmethylene)piperidine; UKMH-111, (3*Z*,5*Z*)-3,5-bis(furan-2-ylmethylene)-1-methylpiperidine; UKMH-112, (3*Z*,5*Z*)-3,5-bis(furan-3-ylmethylene)-1-methylpiperidine; VMAT2, vesicular monoamine transporter; TLC, thin layer chromatography; HPLC, high-performance liquid chromatography; EC, electrochemical detection.

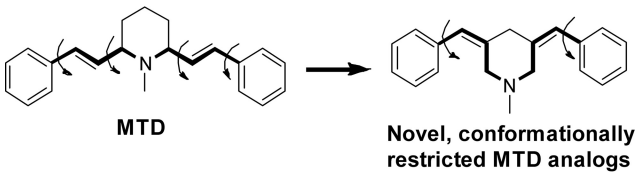


**Fig. 2.** Incorporating the phenylethylene moiety of MTD into the piperdine ring of the analogs affords a novel more rigid molecule. For all analogs in the series, the phenylethylene substituents in the MTD structure (left) were incorporated into the piperidine ring system to afford analogs (right) with a similar number of carbons between the piperidine nitrogen and the phenyl rings. This structural change reduces the molecular weight and the number of rotational carbon bonds (curved arrows) from four in MTD to two in the MTD analogs, affording a novel, more conformationally restricted structure.

analogs of MTD, in which the phenylethylene substituents in the MTD structure were incorporated into the piperidine ring system (Fig. 2). This structural change reduces the molecular weight and the number of rotational carbon bonds from four in MTD to two in the current analogs. Other changes included: 1) altering the geometry of the C5 double bond from E to Z; 2) lengthening the linker units at C3 and C5 of the piperidine ring; 3) adding aromatic substituents to the phenyl moieties; and 4) replacing the phenyl rings with heteroaromatic rings, such as thiophene or furan. Affinity for VMAT2 was retained despite these structural alterations, and importantly, selectivity for VMAT2 was improved. These novel analogs were evaluated further for their ability to inhibit methamphetamine-evoked DA release from superfused rat striatal slices and constitute new leads in the discovery of novel treatments for methamphetamine abuse.

## Materials and Methods

**Animals.** Male Sprague-Dawley rats (200–250 g; Harlan, Indianapolis, IN) were housed two per cage with ad libitum access to food and water in the Division of Laboratory Animal Resources at the University of Kentucky (Lexington, KY). Experimental protocols involving the animals were in accord with the 1996 National Institutes of Health *Guide for the Care and Use of Laboratory Animals* and approved by the Institutional Animal Care and Use Committee at the University of Kentucky.

**Chemicals.** [$^3$H]Nicotine (L-(−)-[*N*-methyl-$^3$H]; specific activity, 66.9 Ci/mmol), [$^3$H]dopamine ([$^3$H]DA; dihydroxyphenylethylamine, 3,4-[7-$^3$H]; specific activity, 28 Ci/mmol), [$^3$H]5-hydroxytryptamine ([$^3$H]5-HT; hydroxytryptamine creatinine sulfate 5-[1,2-$^3$H(N)]; specific activity, 30 Ci/mmol), and Microscint 20 LSC-cocktail were purchased from PerkinElmer Life and Analytical Sciences (Waltham, MA). [$^3$H]Dihydrotetrabenazine ([$^3$H]DTBZ; (±)α-[*O*-methyl-$^3$H]dihydrotetrabenazine; specific activity, 20 Ci/mmol) and [$^3$H]methyllycaconitine ([$^3$H]MLA; ([1α,4(*S*),6β,14α,16β]-20-ethyl-1,6,14,16-tetramethoxy-4-[[[2-([3-$^3$H]-methyl-2,5-dioxo-1-pyrrolidinyl)benzoyl]oxy]-methyl]aconitane-7,8-diol; specific activity, 100 Ci/mmol) were obtained from American Radiolabeled Chemicals, Inc. (St. Louis, MO). Diazepam and ketamine were purchased from N.L.S. Animal Health (Pittsburgh, PA). Acetonitrile, ATP-$Mg^{2+}$, benzaldehyde, 2,4-dichlorobenzaldehyde, 4-methoxybenzaldehyde, 4-methylbenzaldehyde, furan-2-carbaldehyde, furan-3-carbaldehyde, *trans*-cinnamaldehyde, catechol, DA, dihydroxyphenylacetic acid (DOPAC), EDTA, EGTA, ethyl acetate, fluoxetine HCl, 1-(2-(bis-(4-fluorophenyl)methoxy)ethyl)-4-(3-phenylpropyl)piperazine (GBR 12909), α-D-glucose, HEPES, hexane, $MgSO_4$, methanol, methylene chloride, 1-methyl-4-piperidone, pargyline HCl, polyethyleneimine (PEI), KOH, potassium tartrate, sodium borohydride, NaOH, $Na_2SO_4$, sucrose, silica gel (240–400 mesh), and trifluoroacetic acid were purchased from Sigma-Aldrich (St. Louis, MO). L-Ascorbic acid and $NaHCO_3$ were purchased from Aldrich Chemical Co. (Milwaukee, WI). $CaCl_2$, KCl, $K_2PO_4$, $MgCl_2$, NaCl, and $NaH_2PO_4$ were purchased from Fisher Scientific Co. (Pittsburgh, PA). Thiophene-2-carbaldehyde and thiophene-3-carbaldehyde were purchased from Acros Organics (Fairlawn, NJ). Preparative TLC plates (250 μM silica layer, organic binder, no indicator) were purchased from Dynamic Adsorbents Inc. (Atlanta, GA). Chloroform-D was purchased from Cambridge Isotope Laboratories, Inc. (Andover, MA). Complete counting cocktail 3a70B was purchased from Research Products International Corp. (Mt. Prospect, IL). (2*R*,3*S*,11b*S*)-2-ethyl-3-isobutyl-9,10-dimethoxy-2,2,4,6,7,11b-hexahydro-1*H*-pyrido[2,1-a]isoquinolin-2-ol (Ro-4-1284) was a generous gift from Hoffman-LaRoche (Nutley, NJ). MTD was prepared as described by Zheng et al. (2005) and was used as HCl salt.

**General Synthetic Methodology for the UKMH Analogs.** A mixture of 1-methyl-4-piperidone (1.0 eq, 10.2 mmol), the appropriately substituted aromatic aldehyde (2.1 Eq, 21.42 mmol), and potassium hydroxide (2.1 Eq, 21.42 mmol) were stirred in methanol (20 ml) at ambient temperature for 4 h. The resulting yellow precipitate was collected by filtration and washed with cold methanol to yield the crude 3,5-disubstituted-1-methylpiperidin-4-one (9.17–9.83 mmol; 89.9–96.4% yield). Without further purification, the crude 3,5-disubstituted-1-methylpiperidin-4-one product was added to a pre-equilibrated mixture of sodium borohydride (4 Eq) and trifluoroacetic acid (16 Eq) in a 1:1 mixture of dichloromethane and acetonitrile. The mixture was stirred at ambient temperature for 4 to 8 h until TLC and gas chromatography-mass spectroscopy analysis revealed that all of the starting material was consumed. The reaction mixture was then diluted with dichloromethane, and 2 M aqueous sodium hydroxide solution was added drop-wise with stirring to afford a pH of 10. The organic layer was then separated, dried over anhydrous sodium sulfate, and filtered, and the filtrate evaporated to dryness under vacuum. The reaction yielded a mixture of mainly the 3*Z*,5*Z*- and 3*Z*,5*E*-geometrical isomers of the 3,5-disubstituted-1-methylpiperidines, as well as other minor geometric double-bond combinations; both of these isomers could be separated by silica gel column chromatography or preparative TLC, using a 10:1 hexane/ethyl acetate solvent mixture. Using this general procedure, the UKMH series of analogs shown in Fig. 1 were prepared and fully characterized for structural identity and purity, as determined by TLC, gas chromatography-mass spectroscopy, and $^1$H NMR and $^{13}$C NMR analysis. All analogs were converted to HCl salt before analysis.

**Methamphetamine Self-Administration.** Behavioral experiments were conducted as described previously (Neugebauer et al., 2007). Operant conditioning chambers (ENV-008; MED Associates, St. Albans, VT) were enclosed within sound-attenuating compartments (ENV-018M; MED Associates). Each chamber was connected to a personal computer interface (SG-502; MED Associates), and chambers were operated using MED-PC software. A 5 × 4.2-cm recessed food tray was located on the response panel of each chamber. Two retractable response levers were mounted on either side of the recessed food tray (7.3 cm above the metal rod floor). A 28-V, 3-cm diameter, white cue light was mounted 6 cm above each response lever.

Rats were trained briefly to respond on a lever for food reinforcement. Immediately after food training, rats were allowed free access to food for 3 days. Rats were anesthetized (100 mg/kg ketamine and 5 mg/kg diazepam i.p.), and catheters were implanted into the right jugular vein, exiting through a dental acrylic head mount affixed to the skull via jeweler screws. Drug infusions were administered intravenously (0.1 ml over 5.9 s) via a syringe pump (PHM-100; MED Associates) through a water-tight swivel attached to a 10-ml syringe via catheter tubing, which was attached to the cannulae mounted to the head of the rat. After a 1-week recovery period from surgery, rats were trained to press one of two levers for an infusion of methamphetamine (0.05 mg/kg/infusion). Each infusion was followed by a 20-s timeout signaled by illumination of both lever lights. The response requirement was gradually increased to a terminal fixed ratio

5 schedule of reinforcement. Each session was 60 min in duration. Training continued until responding stabilized across sessions. Stable responding was defined as less than 20% variability in the number of infusions earned across three successive sessions, a minimum of a 2:1 ratio of active (drug) lever responses to inactive (no drug) lever responses, and at least 10 infusions per session. Once stability was reached, an acute dose (0, 3.0, 5.6, 10, or 17 mg/kg) of MTD was administered (subcutaneously) 15 min before the session according to a within-subject Latin square design. Two maintenance sessions (i.e., no pretreatment) were included between each test session to ensure stable responding throughout the experiment.

**Food-Maintained Responding.** In brief, rats were trained to respond on one lever (active lever) for food pellet reinforcement (45-mg pellets; BIO-SERV, Frenchtown, NJ), while responses on the other lever (inactive lever) had no programmed consequence. Locations (left or right) of the active and inactive levers were counterbalanced across rats. The response requirement was gradually increased, terminating at fixed ratio 5. After lever training, a 20-s signaled timeout (illumination of both lever lights) was included after each pellet delivery. Timeout after each pellet delivery was instituted to be consistent with the methamphetamine self-administration procedure. Each food-reinforced session lasted 60 min. Training continued until responding stabilized across sessions. Stable responding was defined as less than 20% variability in the number of pellets earned across three successive sessions, and a minimum of a 2:1 ratio of active lever responses to inactive lever responses. After the stability criteria were reached, an acute dose of MTD (17 mg/kg) was administered (subcutaneously) 15 min before the 60-min session. Two maintenance sessions (i.e., no pretreatment) were included between test sessions to ensure stable responding throughout the experiment.

**[$^3$H]Nicotine and [$^3$H]MLA Binding Assays.** Analog-induced inhibition of [$^3$H]nicotine and [$^3$H]MLA binding was determined using published methods (Miller et al., 2004). Whole brain, excluding cortex and cerebellum, was homogenized using a Tekmar polytron (Tekmar-Dohrmann, Mason, OH) in 20 volumes of ice-cold modified Krebs'-HEPES buffer containing 2 mM HEPES, 14.4 mM NaCl, 0.15 mM KCl, 0.2 mM $CaCl_2 \cdot \cdot 2H_2O$, and 0.1 mM $MgSO_4 \cdot 7H_2O$, pH 7.5. Homogenates were centrifuged at 31,000*g* for 17 min at 4°C (Avanti J-301 centrifuge; Beckman Coulter, Fullerton, CA). Pellets were resuspended by sonication (Vibra Cell; Sonics and Materials Inc., Danbury, CT) in 20 volumes of Krebs'-HEPES buffer and incubated at 37°C for 10 min (Reciprocal Shaking Bath model 50; Precision Scientific, Chicago, IL). Suspensions were centrifuged using the above conditions. Resulting pellets were resuspended by sonication in 20 volumes buffer and centrifuged at 31,000*g* for 17 min at 4°C. Final pellets were stored in incubation buffer containing 40 mM HEPES, 288 mM NaCl, 3.0 mM KCl, 4.0 mM $CaCl_2 \cdot 2H_2O$, and 2.0 mM $MgSO_4 \cdot 7H_2O$, pH 7.5. Membrane suspensions (100–140 μg of protein/100 μl) were added to duplicate wells containing 50 μl of analog (7–9 concentrations, 1 nM-0.1 mM, final concentration), 50 μl of buffer, and 50 μl of [$^3$H]nicotine or [$^3$H]MLA (3 nM; final concentration) for a final volume of 250 μl and incubated for 1 h at room temperature. Nonspecific binding was determined in the presence of 10 μM cytisine or 10 μM nicotine for the [$^3$H]nicotine and [$^3$H]MLA assays, respectively. Reactions were terminated by harvesting samples on Unifilter-96 GF/B filter plates presoaked in 0.5% PEI using a Packard Filter Mate Harvester (PerkinElmer Life and Analytical Sciences). Samples were washed three times with 350 μl of ice-cold buffer. Filter plates were dried for 60 min at 45°C and bottom-sealed, and each well was filled with 40 μl of Microscint 20 cocktail. Bound radioactivity was determined via liquid scintillation spectrometry (TopCount NXT scintillation counter; PerkinElmer Life and Analytical Sciences).

**Synaptosomal [$^3$H]DA and [$^3$H]5-HT Uptake Assays.** Analog-induced inhibition of [$^3$H]DA and [$^3$H]5-HT uptake into rat striatal and hippocampal synaptosomes, respectively, was determined using modifications of a previously described method (Teng et al., 1997). Brain regions were homogenized in 20 ml of ice-cold 0.32 M sucrose solution containing 5 mM $NaHCO_3$, pH 7.4, with 16 up-and-down strokes of a Teflon pestle homogenizer (clearance ~ 0.005 inch). Homogenates were centrifuged at 2000*g* for 10 min at 4°C, and resulting supernatants were centrifuged at 20,000*g* for 17 min at 4°C. Pellets were resuspended in 1.5 ml of Krebs' buffer, containing 125 mM NaCl, 5 mM KCl, 1.5 mM $MgSO_4$, 1.25 mM $CaCl_2$, 1.5 mM $KH_2PO_4$, 10 mM α-D-glucose, 25 mM HEPES, 0.1 mM EDTA, with 0.1 mM pargyline and 0.1 mM ascorbic acid saturated with 95% $O_2$/5% $CO_2$, pH 7.4. Synaptosomal suspensions (20 μg of protein/50 μl) were added to duplicate tubes containing 50 μl of analog (7–9 concentrations, 0.1 nM-1 mM, final concentration) and 350 μl of buffer and incubated at 34°C for 5 min in a total volume of 450 μl. Samples were placed on ice and 50 μl of [$^3$H]DA or [$^3$H]5-HT (10 nM; final concentration) was added to each tube for a final volume of 500 μl. Reactions proceeded for 10 min at 34°C and were terminated by the addition of 3 ml of ice-cold Krebs' buffer. Nonspecific [$^3$H]DA and [$^3$H]5-HT uptake were determined in the presence of 10 μM GBR 12909 and 10 μM fluoxetine, respectively. Samples were rapidly filtered through Whatman GF/B filters using a cell harvester (MP-43RS; Brandel Inc., Gaithersburg, MD). Filters were washed three times with 4 ml of ice-cold Krebs' buffer containing catechol (1 μM). Complete counting cocktail was added to the filters and radioactivity was determined by liquid scintillation spectrometry (B1600 TR scintillation counter; PerkinElmer Life and Analytical Sciences).

**[$^3$H]DTBZ Vesicular Binding Assays.** Analog-induced inhibition of [$^3$H]DTBZ binding, a high-affinity ligand for VMAT2, was determined using modifications of a previously published method (Teng et al., 1998). Rat whole brain (excluding cerebellum) was homogenized in 20 ml of ice-cold 0.32 M sucrose solution with 10 up-and-down strokes of a Teflon pestle homogenizer (clearance ~ 0.008 inch). Homogenates were centrifuged at 1000*g* for 12 min at 4°C, and the resulting supernatants were centrifuged at 22,000*g* for 10 min at 4°C. Resulting pellets were osmotically shocked by incubation in 18 ml of cold water for 5 min. Osmolarity was restored by adding 2 ml of 25 mM HEPES and 100 mM potassium tartrate solution. Samples were centrifuged (20,000*g* for 20 min at 4°C), and then 1 mM $MgSO_4$ solution was added to the supernatants. Samples were centrifuged at 100,000*g* for 45 min at 4°C. Pellets were resuspended in cold assay buffer, containing 25 mM HEPES, 100 mM potassium tartrate, 5 mM $MgSO_4$, 0.1 mM EDTA, and 0.05 mM EGTA, pH 7.5. Assays were performed in duplicate in 96-well plates. Vesicular suspensions (15 μg of protein/100 μl) were added to wells containing 50 μl of analog (7–9 concentrations, 0.01 nM-0.1 mM, final concentration), 50 μl of buffer, and 50 μl of [$^3$H]DTBZ (3 nM; final concentration) for a final volume of 250 μl and incubated for 1 h at room temperature. Nonspecific uptake was determined in the presence of 50 μl of 20 μM Ro-4-1284. Reactions were terminated by filtration onto Unifilter-96 GF/B filter plates (presoaked in 0.5% PEI). Filters were washed three times with 350 μl of ice-cold buffer containing 25 mM HEPES, 100 mM potassium-tartrate, 5 mM $MgSO_4$, and 10 mM NaCl, pH 7.5. Filter plates were dried and bottom-sealed and each well was filled with 40 μl of scintillation cocktail (MicroScint 20; PerkinElmer Life and Analytical Sciences). Radioactivity on the filters was determined by liquid scintillation spectrometry.

**Vesicular [$^3$H]DA Uptake Assay.** Analog-induced inhibition of [$^3$H]DA uptake into rat striatal vesicles was determined using modifications of a previously published method (Teng et al., 1997). Previous reports from our laboratory showed that this vesicle preparation contains <1% contaminating membrane fragments (Teng et al., 1997). Striata were homogenized in 14 ml of ice-cold 0.32 M sucrose solution containing 5 mM $NaHCO_3$, pH 7.4, with 10 up-and-down strokes of a Teflon pestle homogenizer (clearance ~ 0.008 inch). Homogenates were centrifuged at 2000*g* for 10 min at 4°C, and the resulting supernatants were centrifuged at 10,000*g* for 30 min at 4°C. Pellets were resuspended in 2.0 ml of 0.32 M sucrose, transferred to tubes containing 7 ml of MilliQ water, and homogenized

with five up-and-down strokes. Homogenates were transferred to tubes containing 900 μl of 0.25 M HEPES and 900 μl of 1.0 M potassium tartrate solution and centrifuged at 20,000*g* for 20 min at 4°C. The resulting supernatants were centrifuged at 55,000*g* for 60 min at 4°C. Subsequently, 100 μl of 1 mM $MgSO_4$, 100 μl of 0.25 M HEPES, and 100 μl of 1.0 M potassium tartrate were added to the supernatant and centrifuged at 100,000*g* for 45 min at 4°C. Final pellets were resuspended in assay buffer containing 25 mM HEPES, 100 mM potassium tartrate, 50 μM EGTA, 100 μM EDTA, 1.7 mM ascorbic acid, and 2 mM ATP-$Mg^{2+}$, pH 7.4. Vesicular suspensions (10 μg of protein/100 μl) were added to duplicate tubes containing 50 μl of analog (7–9 concentrations, 1 nM-0.1 mM, final concentration), 300 μl of buffer, and 50 μl of [$^3$H]DA (0.1 μM; final concentration) for a final volume of 500 μl and incubated for 8 min at 34°C. Nonspecific [$^3$H]DA uptake was determined in the presence of 10 μM Ro-4-1284. Samples were filtered rapidly through Whatman GF/B filters using the cell harvester and washed three times with assay buffer containing 2 mM $MgSO_4$ in the absence of ATP. Radioactivity retained by the filters was determined as described previously.

**Kinetics of Vesicular [$^3$H]DA Uptake.** Vesicle suspensions were prepared as described above; striata were pooled from two rats. Vesicular suspensions (20 μg of protein/50 μl) were added to duplicate tubes containing 25 μl of analog (final concentration approximating the $K_i$), 150 μl of buffer, and 25 μl of [$^3$H]DA (1 nM-5 μM; final concentration) for a final volume of 250 μl and incubated for 8 min at 34°C. Nonspecific [$^3$H]DA uptake was determined in samples containing 10 μM Ro-4-1284. Samples were processed as described previously.

**Endogenous DA Release Assay.** Rat coronal striatal slices (0.5 mm thick) were prepared and incubated in Krebs' buffer containing 118 mM NaCl, 4.7 mM KCl, 1.2 mM $MgCl_2$, 1.0 mM $NaH_2PO_4$, 1.3 mM $CaCl_2$, 11.1 mM α-D-glucose, 25 mM $NaHCO_3$, 0.11 mM L-ascorbic acid, and 0.004 mM EDTA, pH 7.4, saturated with 95% $O_2$/5% $CO_2$ at 34°C in a metabolic shaker for 60 min (Teng et al., 1997). Each slice was transferred to a glass superfusion chamber and superfused at 1 ml/min for 60 min with Krebs' buffer before sample collection. Two basal samples (1 ml) were collected at 5- and 10-min time points. Each slice was superfused for 30 min in the absence or presence of a single concentration of analog (0.1–10 μM) to determine analog-evoked DA and DOPAC overflow and remained in the buffer until the end of the experiment. Methamphetamine (5 μM) was added to the buffer after 30 min of superfusion, and slices were superfused for 15 min, followed by 20 min of superfusion in the absence of methamphetamine. In each experiment, a striatal slice was superfused for 90 min in the absence of both analog and methamphetamine, serving as the buffer control condition. In each experiment, duplicate slices were superfused with methamphetamine in the absence of analog, serving as the methamphetamine control condition. The concentration of methamphetamine was selected based on pilot concentration-response data showing a reliable response of sufficient magnitude to allow evaluation of analog-induced inhibition. Each superfusate sample (1 ml) was collected into tubes containing 100 μl of 0.1 M perchloric acid. Before HPLC-EC analysis, ascorbate oxidase (20 μl, 168 U/mg reconstituted to 81 U/ml) was added to 500 μl of each sample and vortexed for 30 s, and 100 μl of the resulting solution was injected onto the HPLC-EC.

HPLC-EC consisted of a pump (model 126; Beckman Coulter) and autosampler (model 508; Beckman Coulter), an ODS Ultrasphere C18 reverse-phase 80 × 4.6 mm, 3-μm column, and a Coulometric-II detector with guard cell (model 5020) maintained at + 0.60 V and analytical cell (model 5011) maintained at potentials E1 = −0.05 V and E2 = +0.32 V (ESA Inc., Chelmsford, MA). HPLC mobile phase (flow rate, 1.5 ml/min) was 0.07 M citrate/0.1 M acetate buffer, pH 4, containing 175 mg/l octylsulfonic acid sodium salt, 650 mg/l NaCl. and 7% methanol. Separations were performed at room temperature, and 5 to 6 min was required to process each sample. Retention times of DA or DOPAC standards were used to identify respective peaks. Peak heights were used to quantify the detected amounts of analyte based on standard curves. Detection limit for DA and DOPAC was 1 to 2 pg/100 μl.

**Data Analysis.** For the behavioral experiments, one-way ANOVA with dose as a within-subject factor was used to determine whether MTD altered methamphetamine self-administration. Dunnett's post hoc test were used to compare each MTD dose to the saline control. A single paired-sample *t* test was used to determine the effects of MTD on food-maintained behavior.

For the neurochemical experiments, specific [$^3$H]nicotine, [$^3$H]MLA, and [$^3$H]DTBZ binding and specific [$^3$H]DA and [$^3$H]5-HT uptake were determined by subtracting the nonspecific binding or uptake from the total binding or uptake. Analog concentrations producing 50% inhibition of specific binding or uptake ($IC_{50}$ values) were determined from concentration effect curves via an iterative curve-fitting program (Prism 5.0; GraphPad Software Inc., San Diego, CA). Inhibition constants ($K_i$ values) were determined using the Cheng-Prusoff equation (Cheng and Prusoff, 1973). For kinetic analyses, $K_m$ and $V_{max}$ were determined using one-site binding curves. Paired two-tailed *t* tests were performed on the arithmetic $V_{max}$ and the log $K_m$ values to determine significant differences between analog and control conditions. Pearson's correlation analysis determined the relationship between affinity for the [$^3$H]DTBZ binding site and vesicular [$^3$H]DA uptake.

For endogenous neurotransmitter release assays, fractional release was defined as the DA or DOPAC concentration in each sample divided by the slice weight. Basal DA or DOPAC outflow was calculated as the average fractional release of the two basal samples collected 10 min before addition of analog to the buffer. Analog-evoked DA or DOPAC overflow was calculated as the average fractional release during the

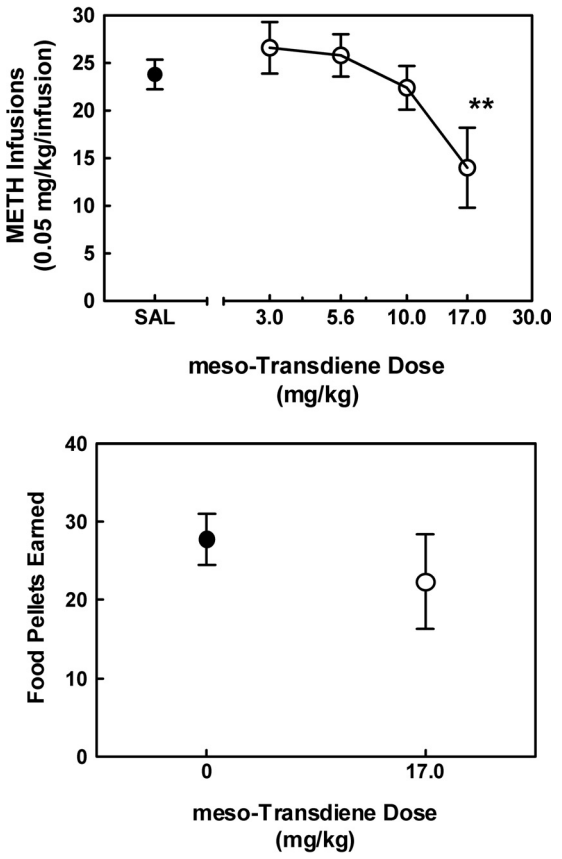


**Fig. 3.** MTD dose-dependently decreases methamphetamine self-administration, without altering food-maintained responding. Top, dose-related effect of acute MTD on methamphetamine (METH) self-administration. Bottom, effect of the high dose of MTD (17.0 mg/kg) on food-maintained responding. Data are expressed as mean ± S.E.M. for number of methamphetamine infusions (0.05 mg/kg/infusion) or number of pellets earned during 60-min sessions ($n$ = 5–6). **, $p < 0.01$ compared with control.

30-min period of analog exposure before methamphetamine addition to the buffer. Analog-evoked DA or DOPAC overflow was analyzed by one-way repeated-measures ANOVA. Time course for analog-induced inhibition of methamphetamine-evoked fractional DA or DOPAC release was analyzed by two-way ANOVA with concentration and time as repeated-measures factors. If a concentration × time interaction was found, one-way ANOVAs were performed at each time point at which methamphetamine-evoked DA release above basal outflow. When appropriate, one-way ANOVAs were followed by Dunnett's post hoc test to determine concentrations of analog that decreased methamphetamine-evoked DA fractional release. Furthermore, one-way ANOVA was performed on the peak response of methamphetamine-evoked fractional release at each analog concentration. The log $IC_{50}$ value was generated using an iterative nonlinear least-squares curve-fitting program (Prism version 5.0). Statistical significance was defined as $p < 0.05$.

## Results

**MTD Decreases Methamphetamine Self-Administration Without Altering Food-Maintained Responding.** The effect of MTD on methamphetamine self-administration is illustrated in Fig. 3, top. One-way ANOVA revealed a dose-related effect of MTD on the number of methamphetamine infusions earned ($F_{4,16} = 4.86$; $p < 0.01$). Dunnett's test revealed that the high dose of MTD (17 mg/kg) decreased the number of methamphetamine infusions earned compared with control. Tolerance developed to the ability of MTD to decrease methamphetamine self-administration on the second day of treatment (data not shown). The effect of the acute high dose of MTD (17 mg/kg) on food-maintained responding is illustrated in Fig. 3, bottom. MTD did not decrease responding for food ($p = 0.414$). Thus, the high dose of MTD specifically decreased methamphetamine self-administration; however, tolerance developed to this effect.

**MTD Analogs Do Not Inhibit [$^3$H]Nicotine and [$^3$H]MLA Binding.** Concentration-response curves and $K_i$ values for lobeline, MTD, and the series of MTD analogs to inhibit [$^3$H]nicotine and [$^3$H]MLA binding to whole brain membranes, compared with nicotine (positive control), are provided in Supplemental Fig. 1 (top and bottom, respectively) and Table 1. $K_i$ values for nicotine were 3 and 370 nM at the [$^3$H]nicotine and [$^3$H]MLA binding sites, respectively, consistent with previous reports (Flammia et al., 1999). $K_i$ values for lobeline were 4 nM and 6.26 μM at the [$^3$H]nicotine and [$^3$H]MLA binding sites, respectively, also consistent with previous reports (Zheng et al., 2005). $K_i$ values for MTD were >100 μM at both [$^3$H]nicotine and [$^3$H]MLA binding sites, as observed previously (Miller et al., 2004). None of the MTD analogs in this series inhibited [$^3$H]nicotine or [$^3$H]MLA binding.

**MTD Analogs Inhibit Synaptosomal [$^3$H]DA Uptake.** Concentration-response curves and $K_i$ values for lobeline, MTD, and the series of MTD analogs to inhibit [$^3$H]DA uptake into striatal synaptosomes, compared with GBR 12909 (positive control), are provided in Fig. 4 and Table 1. The $K_i$ value for GBR 12909 to inhibit [$^3$H]DA uptake was 0.97 nM, consistent with previous reports (Reith et al., 1994). The $K_i$ value for lobeline to inhibit [$^3$H]DA uptake was 28.2 μM, whereas the defunctionalized unsaturated compound MTD exhibited a 200-fold higher potency ($K_i$ = 100 nM) compared with lobeline, in agreement with previous observations (Miller et al., 2004). MTD analogs in the current series exhibited 50- to 1000-fold lower potency ($K_i$ > 5 μM) than MTD at DAT. It is noteworthy that the 2,4-dichlorophenyl analogs, (3*Z*,5*E*)-3,5-bis(2,4-dichlorobenzylidene)-1-methylpiperidine (UKMH-105) and (3*Z*,5*Z*)-3,5-bis(2,4-dichlorobenzylidene)-1-methylpiperidine (UKMH-106), exhibited 60-fold lower potency ($K_i$ = 6.27 and 6.90 μM, respectively) than MTD. Thus, this series of MTD analogs exhibited lower affinities for DAT compared with the parent compound.

**MTD Analogs Inhibit Synaptosomal [$^3$H]5-HT Uptake.** Concentration-response curves and $K_i$ values for lobeline, MTD, and the series of MTD analogs to inhibit [$^3$H]5-HT uptake into hippocampal synaptosomes, compared with fluoxetine (positive control), are provided in Fig. 5 and Table 1. The $K_i$ value for fluoxetine to inhibit [$^3$H]5-HT uptake was 6.5 nM, consistent with previous reports (Owens et al., 2001). The $K_i$ value for lobeline to inhibit [$^3$H]5-HT uptake was 46.8 μM, whereas MTD exhibited 6-fold higher potency ($K_i$ = 7 μM) compared with lobeline, in agreement with previous observations (Miller et al.,

TABLE 1
Affinity values ($K_i$) of MTD analogs, lobeline, MTD, and standard compounds for nicotinic receptors, DAT, SERT, and VMAT2 binding and function

| Compound | [$^3$H]Nicotine Binding $K_i$ ± S.E.M. | [$^3$H]MLA Binding $K_i$ ± S.E.M. | DAT [$^3$H]DA Uptake $K_i$ ± S.E.M. | SERT [$^3$H]5-HT Uptake $K_i$ ± S.E.M. | VMAT2 [$^3$H]DTBZ Binding $K_i$ ± S.E.M. | VMAT2 [$^3$H]DA Uptake $K_i$ ± S.E.M. |
|---|---|---|---|---|---|---|
| | | | μ*M* | | | |
| Nicotine | 0.003 ± 0.0002[a] | 0.37 ± 0.08[a] | N.D. | N.D. | N.D. | N.D. |
| GBR 12909 | N.D. | N.D. | 0.00097 ± 0.0001[a] | N.D. | N.D. | N.D. |
| Fluoxetine | N.D. | N.D. | N.D. | 0.0065 ± 0.0001[a] | N.D. | N.D. |
| Ro-4-1284 | N.D. | N.D. | N.D. | N.D. | 0.028 ± 0.003[a] | 0.018 ± 0.002[a] |
| Lobeline | 0.004 ± 0.0001 | 6.26 ± 1.30 | 28.2 ± 6.73 | 46.8 ± 3.70 | 2.04 ± 0.26[b] | 1.27 ± 0.46 |
| MTD | >100[c] | >100[c] | 0.10 ± 0.01 | 7.00 ± 1.30 | 9.88 ± 2.22[b] | 0.46 ± 0.11 |
| UKMH-101 | >100 | >100 | 11.5 ± 1.90 | 0.71 ± 0.09 | 31.8 ± 5.84 | 0.88 ± 0.19 |
| UKMH-102 | >100 | >100 | 25.1 ± 2.93 | 1.37 ± 0.09 | 12.3 ± 4.70 | 0.22 ± 0.05 |
| UKMH-103 | >100 | >100 | 16.2 ± 1.20 | 2.10 ± 0.51 | 20.3 ± 3.73 | 0.79 ± 0.18 |
| UKMH-104 | >100 | >100 | 5.25 ± 0.46 | 2.67 ± 0.51 | 15.0 ± 5.22 | 0.88 ± 0.26 |
| UKMH-105 | >100 | >100 | 6.27 ± 0.60 | 18.3 ± 7.50 | 4.60 ± 1.70 | 0.22 ± 0.01 |
| UKMH-106 | >100 | >100 | 6.90 ± 1.10 | 20.7 ± 4.90 | 41.3 ± 14.3 | 0.32 ± 0.12 |
| UKMH-107 | >100 | >100 | 68.2 ± 6.93 | 0.51 ± 0.05 | 7.27 ± 2.28 | 1.03 ± 0.19 |
| UKMH-108 | >100 | >100 | 39.0 ± 16.3 | 0.61 ± 0.08 | 3.42 ± 0.26 | 0.33 ± 0.08 |
| UKMH-109 | >100 | >100 | >100 | 16.3 ± 4.10 | 91.3 ± 26.2 | 2.27 ± 1.13 |
| UKMH-110 | >100 | >100 | 58.1 ± 18.7 | 13.4 ± 4.10 | 10.4 ± 2.62 | 0.36 ± 0.12 |
| UKMH-111 | >100 | >100 | >100 | 16.1 ± 2.91 | 32.6 ± 6.79 | 3.82 ± 1.99 |
| UKMH-112 | >100 | >100 | 5.50 ± 0.26 | 0.71 ± 0.19 | 15.5 ± 1.61 | 0.58 ± 0.08 |

N.D., not determined. UKMH-110, (3*Z*,5*Z*)-1-methyl-3,5-bis(thiophen-3-ylmethylene)piperidine; UKMH-111, (3*Z*,5*Z*)-3,5-bis(furan-2-ylmethylene)-1-methylpiperidine.
[a] $n$ = 3–4 rats.
[b] Data taken from Zheng et al., 2005.
[c] Data taken from Miller et al., 2001.

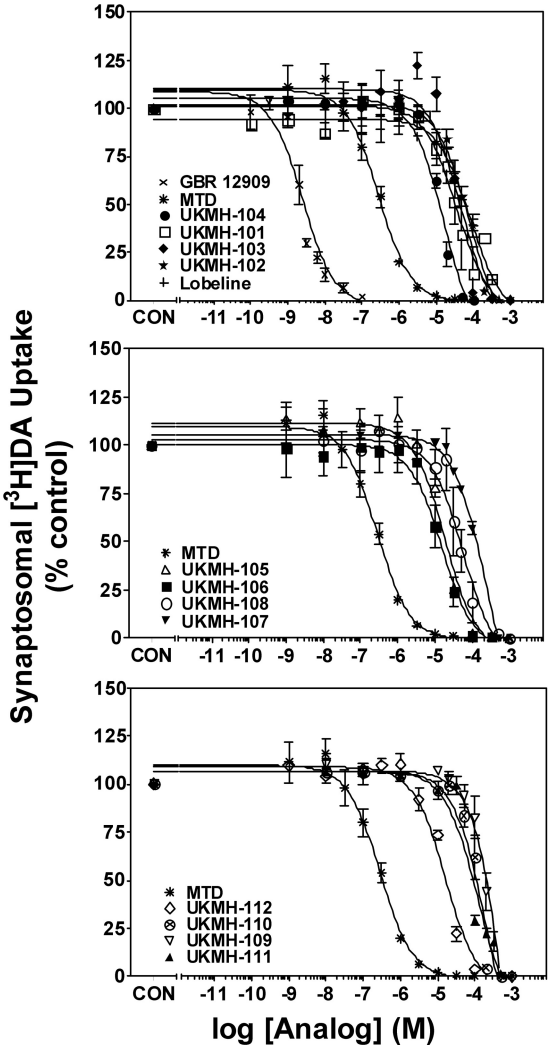


**Fig. 4.** Structural modifications to MTD afford analogs with decreased affinity for DAT. Analogs are grouped according to structural similarity of the aromatic rings. Top, lobeline, MTD, and MTD analogs with no aromatic ring substituents. Middle, MTD analogs with dichloro, methoxy, or methyl aromatic substituents. Bottom, MTD analogs containing heteroaromatic rings. MTD is repeated in all three panels for purpose of comparison. Nonspecific [$^3$H]DA uptake was determined in the presence of 10 μM GBR 12909. Control (CON) represents specific [$^3$H]DA uptake in the absence of analog (35.0 ± 1.55 pmol/mg/min). Legends provide analogs in order from highest to lowest affinity. $n$ = 4 rats/analog.

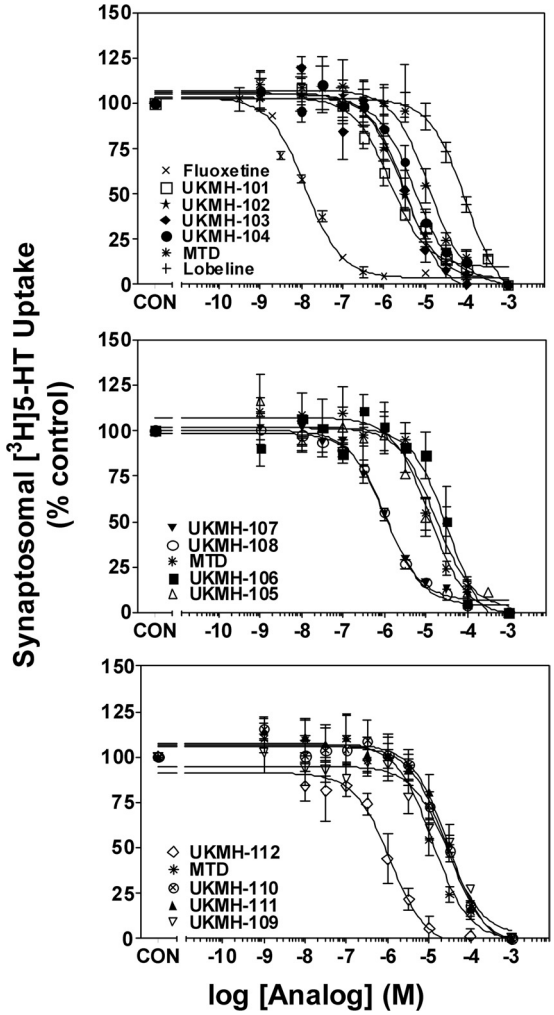


**Fig. 5.** MTD analogs inhibit [$^3$H]5-HT uptake into rat hippocampal synaptosomes. Analogs are grouped according to structural similarity of the aromatic rings. Top, lobeline, MTD, and MTD analogs with no aromatic ring substituents. Middle, MTD analogs with dichloro, methoxy, or methyl aromatic substituents. Bottom, MTD analogs containing heteroaromatic rings. MTD is repeated in all three panels for purpose of comparison. Nonspecific [$^3$H]5-HT uptake was determined in the presence of 10 μM fluoxetine. Control (CON) represents specific [$^3$H]5-HT uptake in the absence of analog (1.67 ± 0.09 pmol/mg/min). Legends provide compounds in order from highest to lowest affinity. $n$ = 4 rats/analog.

2004). The majority of the MTD analogs had $K_i$ values not different from MTD; of note, the 2,4-dichlorophenyl analogs, UKMH-105 and UKMH-106, exhibited low potency at SERT ($K_i$ = 18.3 and 20.7 μM, respectively). Exceptions include (3*Z*,5*E*)-3,5-dibenzylidene-1-methylpiperidine (UKMH-101) (no phenyl substituents), (3*Z*,5*Z*)-3,5-bis(4-methoxybenzylidene)-1-methylpiperidine (UKMH-107) (a 4-methoxyphenyl analog), (3*Z*,5*Z*)-1-methyl-3,5-bis(4-methylbenzylidene)-piperidine (UKMH-108) (a 4-methylphenyl analog), and (3*Z*,5*Z*)-3,5-bis(furan-3-ylmethylene)-1-methylpiperidine (UKMH-112) (a 3-furanyl analog), which exhibited 10-fold higher potency at SERT compared with MTD.

**MTD Analogs Inhibit [$^3$H]DTBZ Binding at VMAT2.** Concentration-response curves and $K_i$ values for lobeline, MTD, and the series of MTD analogs to inhibit [$^3$H]DTBZ binding to whole brain membranes, compared with Ro-4-1284 (positive control), are provided in Fig. 6 and Table 1. The $K_i$ value for Ro-4-1284 to inhibit [$^3$H]DTBZ binding was 28 nM, consistent with a previous report (Cesura et al., 1990). The $K_i$ value for lobeline to inhibit [$^3$H]DTBZ binding was 2.04 μM, whereas MTD exhibited a 5-fold lower potency ($K_i$ = 9.88 nM) compared with lobeline, consistent with previous observations (Zheng et al., 2005). The majority of analogs in the series were equipotent inhibiting [$^3$H]DTBZ binding compared with MTD (Table 1). An exception was (3*Z*,5*Z*)-1-methyl-3,5-bis(thiophen-2-ylmethylene)piperidine (UKMH-109) (2-thiophenyl analog), which exhibited 10-fold lower potency at the [$^3$H]DTBZ binding site compared with MTD. It is noteworthy that UKMH-105 and UKMH-106, the 2,4-dichlorophenyl double-bond isomers, exhibited geometrically specific inhibition of [$^3$H]DTBZ binding ($K_i$ = 4.60 and 41.3 μM, respectively).

**MTD Analogs Inhibit [$^3$H]DA Uptake by VMAT2.** Concentration-response curves and $K_i$ values for lobeline, MTD, and the series of MTD analogs to inhibit [$^3$H]DA uptake into striatal vesicles, compared with Ro-4-1284 (positive control),

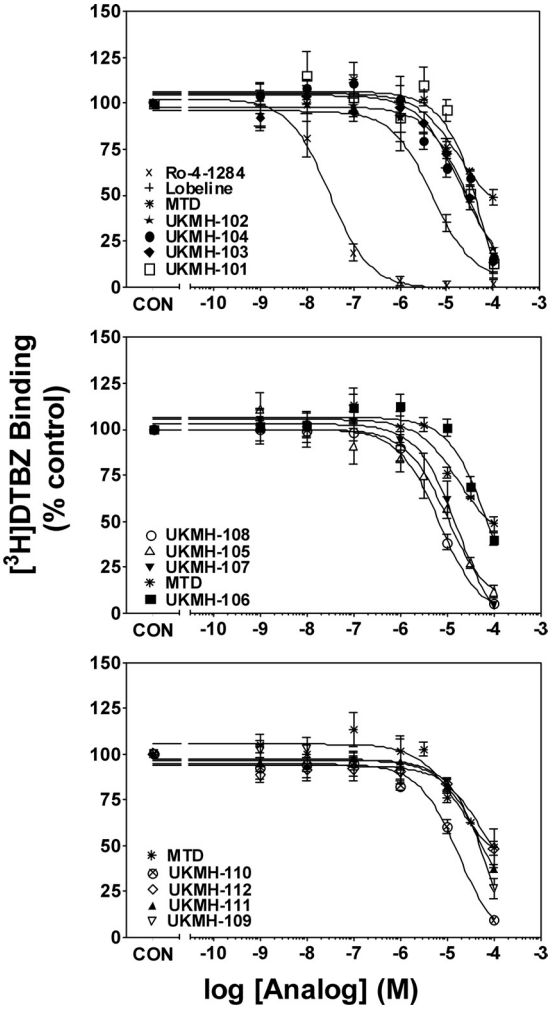


**Fig. 6.** MTD analogs inhibit [$^3$H]DTBZ binding to vesicle membranes from rat whole brain preparations. Analogs are grouped according to structural similarity of the aromatic rings. Top, lobeline, MTD, and MTD analogs with no aromatic ring substituents. Middle, MTD analogs with dichloro, methoxy, or methyl aromatic substituents. Bottom, MTD analogs containing heteroaromatic rings. MTD is repeated in all three panels for purpose of comparison. Nonspecific [$^3$H]DTBZ binding was determined in the presence of 10 μM Ro-4-1284. Control (CON) represents specific [$^3$H]DTBZ binding in the absence of analog (5.01 ± 0.10 pmol/mg protein). Analogs are arranged in order from greatest potency to least potency. $n$ = 4 rats/analog.

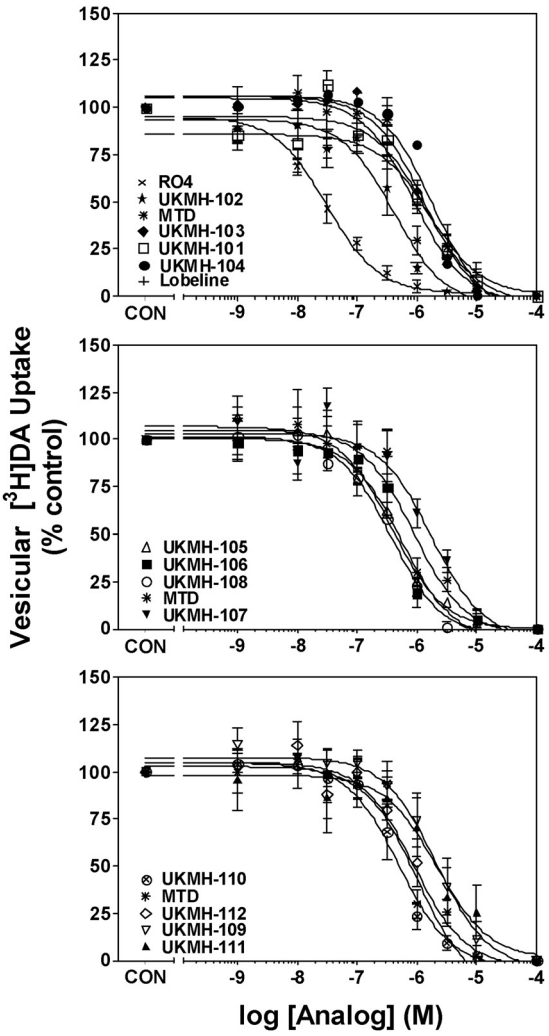


**Fig. 7.** MTD analogs inhibit [$^3$H]DA uptake into rat striatal vesicles. Analogs are grouped according to structural similarity of the aromatic rings. Top, lobeline, MTD, and MTD analogs with no aromatic ring substituents. Middle, MTD analogs with dichloro, methoxy, or methyl aromatic substituents. Bottom, MTD analogs containing heteroaromatic rings. MTD is repeated in all three panels for purpose of comparison. Nonspecific [$^3$H]DA uptake was determined in the presence of 10 μM Ro-4-1284. Control (CON) represents specific vesicular [$^3$H]DA uptake in the absence of analog (29.3 ± 1.38 pmol/mg/min). Legends provide compounds in order from highest to lowest affinity. $n$ = 4 rats/analog.

are provided in Fig. 7 and Table 1. The $K_i$ value for Ro-4-1284 to inhibit [$^3$H]DA uptake was 18 nM, consistent with a previous report (Nickell et al., 2010b). The $K_i$ value for lobeline to inhibit [$^3$H]DA uptake by VMAT2 was 1.27 μM, which was not different from that for MTD ($K_i$ = 0.46 μM), consistent with previous observations (Nickell et al., 2010a). The majority of the analogs in this series were equipotent with MTD inhibiting [$^3$H]DA uptake at VMAT2 (Table 1). It is noteworthy that the 2,4-dichlorophenyl isomers, UKMH-105 and UKMH-106, were two of the most potent analogs in the series, with $K_i$ values of 0.22 and 0.32 μM, respectively.

Figure 8 illustrates $K_i$ values for inhibition of vesicular [$^3$H]DA uptake as a function of $K_i$ for inhibition of [$^3$H]DTBZ binding for lobeline, MTD, and the series of MTD analogs. Correlation analysis revealed no relationship between these parameters probing VMAT2 (Pearson's correlation coefficient $r$ = 0.42; $p$ = 0.13).

**UKMH-105 and UKMH-106 Competitively Inhibit [$^3$H]DA Uptake at VMAT2.** UKMH-105 and UKMH-106 were 20- to 450-fold selective for VMAT2 over DAT, SERT, and α4β2* and α7* nAChRs (* indicates putative nAChR subtype assignment). UKMH-105 and UKMH-106 had 10- to 100-fold higher affinity in the VMAT2 functional assay compared with the VMAT2 binding assay. To further evaluate these two analogs, kinetic analyses of [$^3$H]DA uptake at VMAT2 were conducted to determine the mechanism of inhibition, i.e., competitive or noncompetitive, compared with parent compounds (MTD and lobeline). Kinetic assays revealed an increased $K_m$ value and no change in $V_{max}$ for each compound (Fig. 9) compared with control, indicating a competitive mechanism of action.

**UKMH-106 Inhibits Methamphetamine-Evoked Endogenous DA Release, Whereas UKMH-105 Does Not.** The ability of UKMH-105 and UKMH-106 to evoke DA release

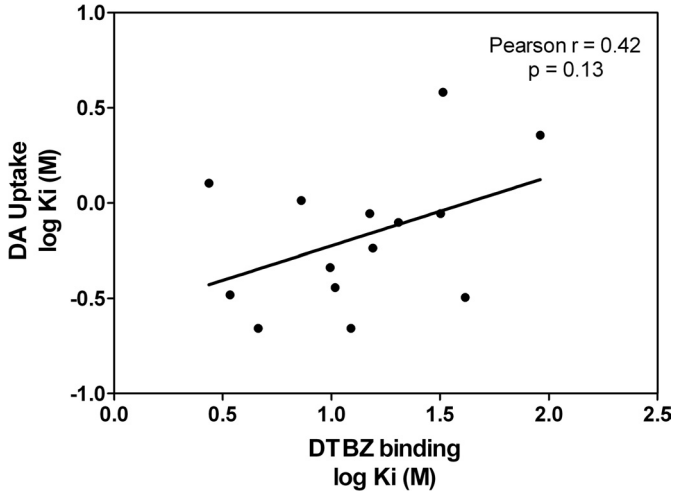


**Fig. 8.** Inhibition of [$^3$H]DTBZ binding does not predict inhibition of [$^3$H]DA uptake at VMAT2. Data presented are $K_i$ values from analog-induced inhibition of [$^3$H]DTBZ binding and [$^3$H]DA uptake at VMAT2 (Figs. 6 and 7, respectively). Pearson's correlation analysis of these data revealed a lack of correlation (Pearson's $r = 0.42$; $p = 0.13$) between the ability of analogs to inhibit [$^3$H]DTBZ binding and [$^3$H]DA uptake at VMAT2.

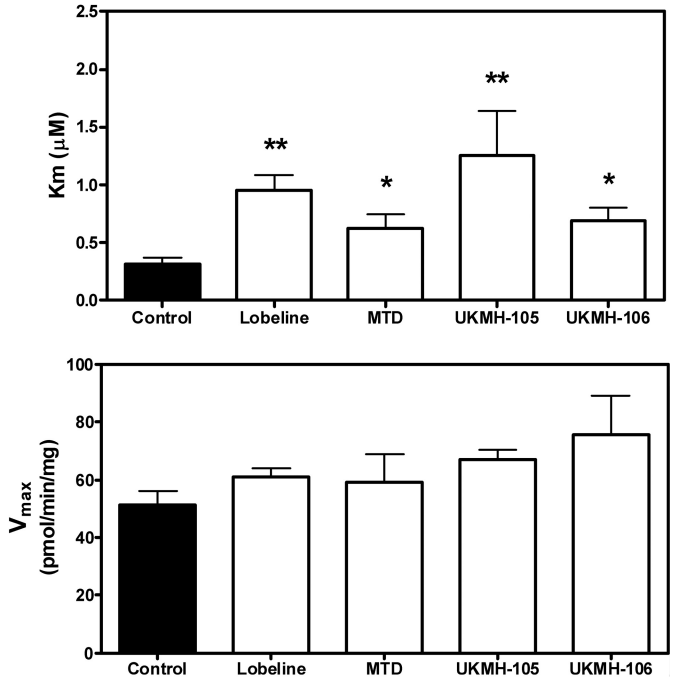


**Fig. 9.** Lobeline, MTD, and MTD analogs competitively inhibit [$^3$H]DA uptake into vesicles prepared from rat striatum. Concentrations of lobeline (0.25 μM), MTD (0.23 μM), UKMH-105 (0.11 μM), and UKMH-106 (0.16 μM) approximated the $K_i$ values for inhibiting [$^3$H]DA uptake into isolated synaptic vesicles obtained from the data shown in Fig. 7. $K_m$ (top) and $V_{max}$ (bottom) values are mean ± S.E.M. *, $p < 0.05$ different from control; **, $p < 0.01$ different from control. $n = 4$–7 rats/analog).

from superfused striatal slices is illustrated in Figs. 10 and 11. Analysis of the effect of UKMH-105 on DA release before the addition of methamphetamine to the buffer (20–40 min of sample collection) showed no main effects of concentration ($F_{5,29} = 0.47$; $p > 0.05$) and time ($F_{4,29} = 1.01$; $p > 0.05$) and no concentration × time interaction ($F_{20,29} = 0.67$; $p > 0.05$). Thus, UKMH-105 alone did not evoke DA release. Likewise, UKMH-106 did not alter DA release [no main effect of concentration

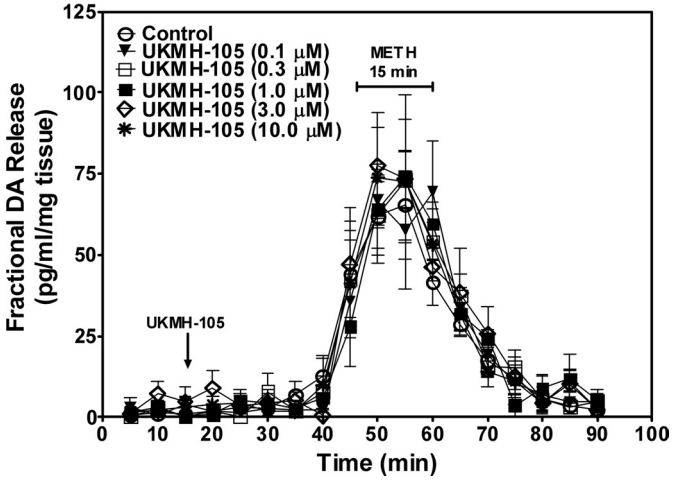


**Fig. 10.** UKMH-105 does not inhibit methamphetamine-evoked endogenous DA release from striatal slices. Fractional DA release represents the amount of DA in each 5-min sample. Slices were superfused with UKMH-105 after 10-min collection of basal samples, as indicated by the arrow, and analog remained in the buffer until the end of the experiment. Methamphetamine (METH; 5 μM) was added to the buffer for 15 min as indicated by the horizontal bar. Fractional release data are expressed as mean ± S.E.M. pg/ml/mg of the slice weight. $n = 5$ rats.

($F_{4,43} = 0.12$; $p > 0.05$) and showed no time × concentration interaction ($F_{16,43} = 1.57$; $p > 0.05$)]. A main effect of time was found ($F_{4,43} = 6.78$, $p < 0.05$), revealing that fractional release increased slightly across the 20-min exposure period in both the absence and presence of UKMH-106. Both UKMH-105 and UKMH-106 also had no effect on DOPAC fractional release across this time period (data not shown).

The ability of UKMH-105 and UKMH-106 to decrease methamphetamine-evoked DA release is illustrated in Figs. 10 and 11. A two-way repeated measures ANOVA on fractional DA release during exposure to UKMH-105 and methamphetamine revealed no main effect of concentration ($F_{5,29} = 0.65$; $p > 0.05$) and no concentration × time interaction ($F_{25,29} = 0.45$; $p > 0.05$); however, a main effect of time ($F_{5,29} = 15.4$, $p < 0.0001$) was observed, which reflects the increase in fractional release evoked by methamphetamine in the absence and presence of UKMH-105. Similarly, only a main effect of time was found for DOPAC superfusate concentrations; although in the absence and presence of UKMH-105, DOPAC fractional release was decreased in response to methamphetamine (data not shown). Thus, UKMH-105 did not alter the effect of methamphetamine on DA or DOPAC fractional release.

In a concentration-dependent manner, UKMH-106 decreased DA release evoked by methamphetamine (Fig. 11). Two-way repeated-measures ANOVA on fractional DA release during exposure to UKMH-106 and methamphetamine revealed a main effect of concentration ($F_{4,43} = 7.61$; $p < 0.0001$) and time ($F_{5,43} = 23.0$; $p < 0.0001$) and a concentration × time interaction ($F_{20,43} = 1.68$; $p < 0.05$). Post hoc analysis revealed that UKMH-106 (1.0 and 3.0 μM) decreased methamphetamine-evoked DA release compared with control at 50 to 55 min and 50 to 60 min, respectively. The concentration response for UKMH-106 to inhibit methamphetamine-evoked DA release at peak response is illustrated in Fig. 11. $IC_{50}$ and $I_{max}$ values were 0.38 ± 0.13 μM and 50.2 ± 15.5%, respectively. One-way ANOVA on peak response data revealed a concentration-dependent effect of UKMH-106 ($F_{4,43} = 3.11$; $p < 0.05$). Post hoc

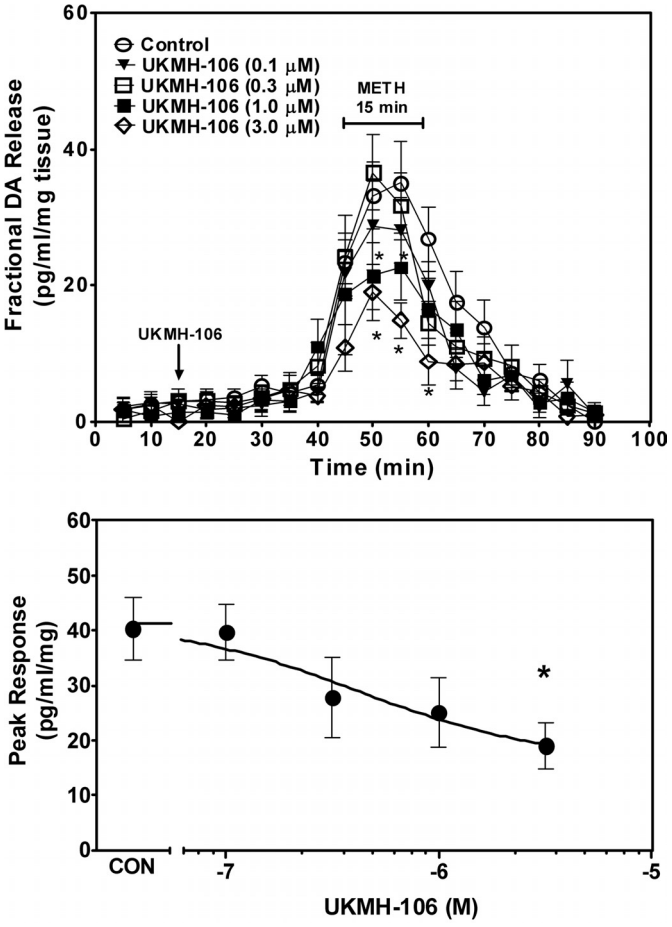


**Fig. 11.** In a concentration-dependent manner, UKMH-106 inhibits methamphetamine-evoked DA release in striatal slices. Top, fractional DA release represents the amount of DA in each 5-min sample. Slices were superfused with UKMH-106 after 10-min collection of basal samples, as indicated by the arrow, and analog remained in the buffer until the end of the experiment. Methamphetamine (METH; 5 μM) was added to the buffer for 15 min as indicated by the horizontal bar. Bottom, concentration-response curve was derived from peak response data for each concentration of UKMH-106. Fractional release and peak response data are expressed as mean ± S.E.M. pg/ml/mg of the slice weight. For fractional release, *, $p < 0.05$ different from methamphetamine alone. For peak response, *, $p < 0.05$ different from peak response of methamphetamine alone (CON). $n = 8$ rats.

analysis revealed that 3 μM UKMH-106 inhibited the DA peak response. In contrast to the ability of UKMH-106 to decrease methamphetamine-evoked fractional DA release, fractional DOPAC release was not altered (data not shown).

## Discussion

In the current study, MTD was shown to decrease methamphetamine self-administration specifically, but only at the highest dose evaluated, and tolerance developed rapidly to this effect. Taking into account this encouraging finding, but tempered by the limitations associated with the development of tolerance, modifications to the MTD molecule were evaluated in search of preclinical candidates for the treatment of methamphetamine abuse. SAR identified several conformationally restricted MTD analogs with high affinity and selectivity for VMAT2. Structural modifications included lengthening the linker units, introduction of 4-methoxy, 4-methyl, or 2,4-dichloro substituents into the phenyl rings, or replacement of the phenyl rings with thiophene or furan rings. Effects of altering the geometry of the double bond at the C5-position of the piperidine ring were evaluated in analogs with either a lengthened linker unit or an aromatic 2,4-dichloro substituted phenyl ring. Affinity for VMAT2 was retained, and increases in selectivity for VMAT2 over DAT were found. The most selective analogs inhibited methamphetamine-evoked DA release in a geometrically specific manner.

Conformational restriction in combination with both *E* and *Z* geometries at the C5 position of the piperidine ring [UKMH-101 and (3*Z*,5*Z*)-3,5-dibenzylidene-1-methylpiperidine (UKMH-102), respectively] did not alter affinity for VMAT2 binding and uptake sites. Lengthening the linker units, regardless of *E* or *Z* geometry [(3*Z*,5*E*)-1-methyl-3,5-bis((*E*)-3-phenylallylidene)piperidine (UKMH-103) and (3*Z*,5*Z*)-1-methyl-3,5-bis((*E*)-3-phenylallylidene)piperidine (UKMH-104), respectively], or adding aromatic 4-methoxy or 4-methyl substituents (UKMH-107 and UKMH-108, respectively), did not alter VMAT2 binding and function. Adding aromatic electron-withdrawing 2,4-dichloro groups in combination with *E* or *Z* geometries at the C5-postion on the piperidine ring (UKMH-105 and UKMH-106, respectively) afforded equipotent inhibition of uptake compared with MTD. In kinetic analyses, UKMH-105 and UKMH-106 increased $K_m$ and did not alter $V_{max}$, indicating competitive inhibition of DA uptake. Although no differences in affinity for VMAT2 uptake sites were observed, geometrically specific inhibition of [$^3$H]DTBZ binding was observed. Specifically, UKMH-106 (3*Z*,5*Z* geometry) had 10-fold lower affinity than UKMH-105 (3*Z*,5*E* geometry) at the [$^3$H]DTBZ binding site. In contrast, double-bond geometry was not a contributing factor to affinity for VMAT2 binding or uptake in analogs (UKMH-101 and UKMH-102) with no phenyl ring substituents or analogs (UKMH-103 and UKMH-104) with lengthened linker units and no phenyl ring substituents. Although *E* geometry was better tolerated than *Z* geometry at the VMAT2 binding site, double-bond geometry was not a factor for affinity at the VMAT2 uptake site.

Substitution of the phenyl rings with thiophene or furan moieties afforded analogs with equipotent or 10-fold lower affinity for VMAT2 binding and uptake sites, compared with MTD. Substitution position on the heteroaromatic ring was a factor influencing affinity. Specifically, 3-substituted analogs were equipotent at VMAT2 binding and uptake sites compared with MTD, whereas 2-substituted analogs exhibited 10-fold lower potency. These results suggest that VMAT2 can accommodate analogs in which furanyl and thiophenyl rings have been substituted for phenyl rings, with the 3-positional isomer better tolerated than the 2-positional isomer.

The current results provide examples of structural modifications that dissociate affinity for the VMAT2 binding site from that for the VMAT2 substrate site and support previous observations showing a lack of correlation between affinities for these sites (Nickell et al., 2010b). The best examples from the current series of analogs are the 2,4-dichlorophenyl analogs (UKMH-105 and UKMH-106), which were equipotent at the VMAT2 uptake site, yet exhibited a 10-fold difference in affinity at the VMAT2 binding site. Thus, these findings support an interaction at two alternate sites on VMAT2 associated with distinct pharmacophores.

One goal of this study was to discover MTD analogs with greater selectivity for VMAT2 over DAT. MTD had low affin-

ity ($K_i$ >100 μM) at α4β2* and α7* nAChRs and inhibited DA uptake by DAT ($K_i$ = 500 nM) and 5-HT uptake by SERT ($K_i$ = 8.9 μM) (Miller et al., 2004). Psychostimulant-induced inhibition of DAT function resulted in increases in extracellular DA, leading to reward and abuse (Ritz et al., 1987; Williams and Galli, 2006). Affinity of MTD for DAT ($K_i$ = 100 nM; current study) is similar to that for cocaine and methylphenidate ($K_i$ = 300 and 100 nM, respectively) (Han and Gu, 2006), suggesting that MTD may have abuse liability. Reducing affinity for DAT is imperative to avoiding abuse liability. Analogs in the current series had reduced affinity (50- to 1000-fold) at DAT compared with MTD. Substitution of the phenyl rings with 3-thiophenyl and 3-furanyl rings resulted in the greatest decreases in DAT affinity. Thus, the current analogs have increased selectivity for VMAT2 over DAT, compared with MTD, and would be predicted to have reduced abuse liability.

Because MTD had moderate affinity for SERT (Miller et al., 2004), affinity of the MTD analogs for SERT also was evaluated. Introduction of aromatic 4-methoxy or 4-methyl substituents into the phenyl rings of MTD resulted in a 5- to 10-fold increased affinity for SERT compared with MTD. The remaining structural changes to MTD did not alter affinity at SERT compared with MTD.

Because the 2,4-dichlorophenyl analogs, UKMH-105 and UKMH-106, exhibited high affinity and selectivity for inhibiting VMAT2 function, these compounds were evaluated for their ability to decrease methamphetamine-evoked DA release. Alone these analogs did not evoke DA release. UKMH-106, but not UKMH-105, inhibited methamphetamine-evoked DA release. Inhibition of DA uptake by the analogs at the VMAT2 substrate site does not explain the C5 *Z*-selective inhibition of the effect of methamphetamine on VMAT2. UKMH-105 and UKMH-106 equipotently inhibited DA uptake by VMAT2, but exhibited C5 *Z*-selective inhibition of methamphetamine-evoked DA release, suggesting that these two geometrical isomers interact with different sites on VMAT2 to inhibit DA uptake and methamphetamine-evoked DA release. Only, the *Z* double-bond geometry at the C5 position of the piperidine ring (UKMH-106) was tolerated by the DA release site, whereas the DA uptake site also tolerated the C5 *E* geometry (UKMH-105). Thus, the VMAT2 site mediating methamphetamine-evoked DA release is restricted in its ability to accommodate both geometrical isomers compared with the VMAT2 uptake site.

Although the mechanism by which methamphetamine releases DA from synaptic vesicles is not understood fully, potential mechanisms include weak base effects of methamphetamine, which disrupt vesicular proton gradients and methamphetamine effects at the VMAT2 substrate site (Sulzer et al., 2005). Although having different double-bond geometries, UKMH-105 and UKMH-106 are expected to have comparable p$K_a$ values, inconsistent with the weak base hypothesis as an explanation for differential effects in decreasing methamphetamine-evoked DA release. However, current observations are consistent with previous reports showing differential effects of the amphetamine optical isomers (Arnold et al., 1977; Fischer and Cho, 1979), despite having identical p$K_a$ values, which again does not support the weak base hypothesis (Sulzer et al., 2005). Thus, UKMH-106 may inhibit methamphetamine-evoked DA release through an interaction with VMAT2 and not via a weak-base mechanism.

One caveat of the current study is that inhibitory effects of the analogs on DA uptake and methamphetamine-evoked DA release were evaluated using different preparations (i.e., isolated vesicles and more intact slices, respectively). One alternative explanation is that the analogs may inhibit methamphetamine-evoked DA release by interacting with DAT in the slice. Cytosolic DA is transported to the extracellular compartment through a methamphetamine-induced reversal of DAT (Fischer and Cho, 1979). However, UKMH-106 inhibited methamphetamine-evoked DA release 18-fold more potently than inhibition of DAT function, making it unlikely that inhibition of DAT is responsible for the decrease in methamphetamine-evoked DA release. If inhibition of DAT was responsible, then both UKMH-105 and UKMH-106 would be expected to decrease methamphetamine-evoked DA release, because they are equipotent inhibiting DAT.

A concern regarding the approach of developing VMAT2 inhibitors as treatments for methamphetamine abuse is the potential for neurotoxicity, because increased cytosolic DA levels can lead to oxidative stress. Methamphetamine inhibits DA uptake at VMAT2, promotes DA release from vesicles, inhibits monoamine oxidase, and produces DA deficits caused by increased formation of reactive oxygen species (Fleckenstein et al., 2007). To the contrary, lobeline protects against methamphetamine-induced neurotoxicity (Eyerman and Yamamoto, 2005). Furthermore, methamphetamine-addicted individuals given lobeline in phase I clinical trials exhibited no adverse effects (http://www.clinicaltrials.gov/ct2/show/NCT00439504?term=NCT00439504&rank=1), and tetrabenazine (a classic VMAT2 inhibitor) is approved by the Food and Drug Administration for the treatment of Huntington's chorea (Frank, 2010). Thus, precedent for the clinical use of VMAT2 inhibitors exists. Nevertheless, evaluation of the potential neurotoxicity of these analogs using animal models will be an integral component of the drug development process for these candidate treatments for methamphetamine abuse.

In summary, the current results extend our previous research by showing that MTD decreases methamphetamine self-administration without altering food-maintained responding, demonstrating that inhibition of VMAT2 function translates to a promising behavioral result. However, MTD has relatively low water solubility and diminishing drug likeness and has high affinity (100 nM) for DAT, which may result in abuse liability. Current results show that incorporation of the phenylethylene moiety of MTD into the piperidine ring system, and the addition of aromatic dichloro substituents, results in a novel candidate compound, UKMH-106, which has improved water solubility and reduced affinity for DAT, SERT, and nAChRs, thereby increasing selectivity for VMAT2. Moreover UKMH-106 decreased the effect of methamphetamine to evoke DA release. Thus, the current research using a classic pharmacological approach has identified a novel lead compound that shows promise as a pharmacotherapy to treat methamphetamine abuse, a devastating problem for which there are no available treatments.

**Authorship Contributions**

*Participated in research design:* Horton, Hojahmat, Bardo, Crooks, and Dwoskin.

*Conducted experiments:* Horton, Siripurapu, Norrholm, Beckmann, Harrod, and Deaciuc.

*Contributed new reagents or analytic tools:* Culver, Hojahmat, and Crooks.

*Performed data analysis:* Horton, Siripurapu, Norrholm, Culver, Hojahmat, Beckmann, Harrod, Deaciuc, Crooks, and Dwoskin.

*Wrote or contributed to the writing of the manuscript:* Horton, Bardo, Crooks, and Dwoskin.

**References**


Arnold EB, Molinoff PB, and Rutledge CO (1977) The release of endogenous norepinephrine and dopamine from cerebral cortex by amphetamine. *J Pharmacol Exp Ther* **202:**544–557.

Beckmann JS, Siripurapu KB, Nickell JR, Horton DB, Denehy ED, Vartak A, Crooks PA, Dwoskin LP, and Bardo MT (2010) The novel pyrrolidine nor-lobelane analog UKCP-110 [*cis*-2,3-di-(2-phenethyl)-pyrrolidine hydrochloride] inhibits VMAT2 function, methamphetamine-evoked dopamine release and methamphetamine self-administration in rats. *J Pharmacol Exp Ther* **335:**841–851.

Cesura AM, Bertocci B, and Da Prada M (1990) Binding of [$^{3}$H]dihydrotetrabenazine and [$^{125}$I]azidoiodoketanserin photoaffinity labeling of the monoamine transporter of platelet 5-HT organelles. *Eur J Pharmacol* **186:**95–104.

Cheng Y and Prusoff WH (1973) Relationship between the inhibition constant (KI) and the concentration of inhibitor which causes 50 percent inhibition (I50) of an enzymatic reaction. *Biochem Pharmacol* **22:**3099–3108.

Damaj MI, Patrick GS, Creasy KR, and Martin BR (1997) Pharmacology of lobeline, a nicotinic receptor ligand. *J Pharmacol Exp Ther* **282:**410–419.

Dar DE, Thiruvazhi M, Abraham P, Kitayama S, Kopajtic TA, Gamliel A, Slusher BS, Carroll FI, and Uhl GR (2005) Structure-activity relationship of trihexyphenidyl analogs with respect to the dopamine transporter in the ongoing search for a cocaine inhibitor. *Eur J Med Chem* **40:**1013–1021.

Di Chiara G and Imperato A (1988) Drugs abused by humans preferentially increase synaptic dopamine concentrations in the mesolimbic system of freely moving rats. *Proc Natl Acad Sci USA* **85:**5274–5278.

Di Chiara G, Bassareo V, Fenu S, De Luca MA, Spina L, Cadoni C, Acquas E, Carboni E, Valentini V, and Lecca D (2004) Dopamine and drug addiction: the nucleus acumens shell connection. *Neuropharmacology* **47:**227–241.

Eyerman DJ and Yamamoto BK (2005) Lobeline attenuates methamphetamine-induced changes in vesicular monoamine transporter-2 immunoreactivity and monoamine depletions in the striatum. *J Pharmacol Exp Ther* **312:**160–169.

Flammia D, Dukat M, Damaj MI, Martin B, and Glennon RA (1999) Lobeline: structure-affinity investigation of nicotinic acetylcholinergic receptor binding. *J Med Chem* **42:**3726–3731.

Fleckenstein AE, Volz TJ, Riddle EL, Gibb JW, and Hanson GR (2007) New insights into the mechanism of action of amphetamines. *Annu Rev Pharmacol Toxicol* **47:**681–698.

Fischer JF and Cho AK (1979) Chemical release of dopamine from striatal homogenates: evidence for an exchange diffusion model. *J Pharmacol Exp Ther* **208:**203–209.

Frank S (2010) Tetrabenazine: the first approved drug for the treatment of chorea in US patients with Huntington disease. *Neuropsychiatr Dis Treat* **6:**657–665.

Han DD and Gu HH (2006) Comparison of the monoamine transporters from human and mouse in their sensitivities to psychostimulant drugs. *BMC Pharmacol* **6:**6.

Harrod SB, Dwoskin LP, Crooks PA, Klebaur JE, and Bardo MT (2001) Lobeline attenuates D-methamphetamine self-administration in rats. *J Pharmacol Exp Ther* **298:**172–179.

Harrod SB, Dwoskin LP, Green TA, Gehrke BJ, and Bardo MT (2003) Lobeline does not serve as a reinforcer in rats. *Psychopharmacology* **165:**397–404.

Howell LL, Carroll FI, Votaw JR, Goodman MM, and Kimmel HL (2007) Effects of combined dopamine and serotonin transporter inhibitors on cocaine self-administration in rhesus monkeys. *J Pharmacol Exp Ther* **320:**757–765.

Kilbourn M, Lee L, Vander Borght T, Jewett D, and Frey K (1995) Binding of α-dihydrotetrabenazine to the vesicular monoamine transporter is stereoselective. *Eur J Pharmacol* **278:**249–252.

Liang NY and Rutledge CO (1982) Evidence for carrier-mediated efflux of dopamine from corpus striatum. *Biochem Pharmacol* **31:**2479–2484.

Miller DK, Crooks PA, and Dwoskin LP (2000) Lobeline inhibits nicotine-evoked [$^{3}$H]dopamine overflow from rat striatal slices and nicotine-evoked $^{86}Rb^{+}$ efflux from thalamic synaptosomes. *Neuropharmacology* **39:**2654–2662.

Miller DK, Crooks PA, Teng L, Witkin JM, Munzar P, Goldberg SR, Acri JB, and Dwoskin LP (2001) Lobeline inhibits the neurochemical and behavioral effects of amphetamine. *J Pharmacol Exp Ther* **296:**1023–1034.

Miller DK, Crooks PA, Zheng G, Grinevich VP, Norrholm SD, and Dwoskin LP (2004) Lobeline analogs with enhanced affinity and selectivity for plasmalemma and vesicular monoamine transporters. *J Pharmacol Exp Ther* **310:**1035–1045.

Neugebauer NM, Harrod SB, Stairs DJ, Crooks PA, Dwoskin LP, and Bardo MT (2007) Lobelane decreases methamphetamine self-administration in rats. *Eur J Pharmacol* **571:**33–38.

Nickell JR, Krishnamurthy S, Norrholm S, Deaciuc G, Siripurapu KB, Zheng G, Crooks PA, and Dwoskin LP (2010a) Lobelane inhibits methamphetamine-evoked dopamine release via inhibition of the vesicular monoamine transporter-2. *J Pharmacol Exp Ther* **332:**612–621.

Nickell JR, Zheng G, Deaciuc AG, Crooks PA, and Dwoskin LP (2010b) Phenyl ring-substituted lobelane analogs: inhibition of [$^{3}$H]dopamine uptake at the vesicular monoamine transporter-2. *J Pharmacol Exp Ther* doi:10.1124/jpet.110.172882.

Owens MJ, Knight DL, and Nemeroff CB (2001) Second-generation SSRIs: human monoamine transporter binding profile of escitalopram and *R*-fluoxetine. *Biol Psychiatry* **50:**345–350.

Pifl C, Drobny H, Reither H, Hornykiewicz O, and Singer EA (1995) Mechanism of the dopamine-releasing actions of amphetamine and cocaine: plasmalemmal dopamine transporter versus vesicular monoamine transporter. *Mol Pharmacol* **47:**368–373.

Reith ME, Coffey LL, Xu C, and Chen NH (1994) GBR 12909 and 12935 block dopamine uptake into brain synaptic vesicles as well as nerve endings. *Eur J Pharmacol* **253:**175–178.

Ritz MC, Lamb RJ, Goldberg SR, and Kuhar MJ (1987) Cocaine receptors on dopamine transporters are related to self-administration of cocaine. *Science* **237:**1219–1223.

Substance Abuse and Mental Health Services Administration, Office of Applied Studies (2008) *Results from the 2007 National Survey on Drug Use and Health: National Findings* (National Survey on Drug Use and Health Series H-34, Department of Health and Human Services Publication SMA 08-4343), National Survey on Drug Use and Health, Rockville, MD.

Sulzer D and Rayport S (1990) Amphetamine and other psychostimulants reduce pH gradients in midbrain dopaminergic neurons and chromaffin granules: a mechanism of action. *Neuron* **5:**797–808.

Sulzer D, Chen TK, Lau YY, Kristensen H, Rayport S, and Ewing A (1995) Amphetamine redistributes dopamine from synaptic vesicles to the cytosol and promotes reverse transport. *J Neurosci* **15:**4102–4108.

Sulzer D, Sonders MS, Poulsen NW, and Galli A (2005) Mechanisms of neurotransmitter release by amphetamines: a review. *Prog Neurobiol* **75:**406–433.

Tanda G, Newman AH, and Katz JL (2009) Discovery of drugs to treat cocaine dependence: behavioral and neurochemical effects of atypical dopamine transport inhibitors. *Adv Pharmacol* **57:**253–289.

Teng L, Crooks PA, and Dwoskin LP (1998) Lobeline displaces [$^{3}$H]dihydrotetrabenazine binding and releases [$^{3}$H]dopamine from rat striatal synaptic vesicles: comparison with D-amphetamine. *J Neurochem* **71:**258–265.

Teng L, Crooks PA, Sonsalla PK, and Dwoskin LP (1997) Lobeline and nicotine evoke [$^{3}$H]overflow from rat striatal slices preloaded with [$^{3}$H]dopamine: differential inhibition of synaptosomal and vesicular [$^{3}$H]dopamine uptake. *J Pharmacol Exp Ther* **280:**1432–1444.

Williams JM and Galli A (2006) The dopamine transporter: a vigilant border control for psychostimulant action. *Handb Exp Pharmacol* **175:**215–232.

Wise RA and Bozarth MA (1987) A psychomotor stimulant theory of addiction. *Psychol Rev* **94:**469–492.

Zheng G, Dwoskin LP, Deaciuc AG, Norrholm SD, and Crooks PA (2005) Defunctionalized lobeline analogues: structure-activity of novel ligands for the vesicular monoamine transporter. *J Med Chem* **48:**5551–5560.


**Address correspondence to:** Dr. Linda Dwoskin, College of Pharmacy, University of Kentucky, Lexington, KY 40536-0082. E-mail: ldwoskin@email.uky.edu